Biomaterials 34 (2013) 2822–2833

Contents lists available at SciVerse ScienceDirect

Biomaterials

journal homepage: www.elsevier.com/locate/biomaterials

A molecular dynamics simulation study on the effect of lipid substitution on polyethylenimine mediated siRNA complexation

Chongbo Sun [a], Tian Tang [a,*], Hasan Uludag [b,c,d]

[a] Department of Mechanical Engineering, University of Alberta, Edmonton, AB T6G 2G8, Canada
[b] Department of Chemical and Materials Engineering, University of Alberta, Edmonton, AB T6G 2G8, Canada
[c] Department of Biomedical Engineering, University of Alberta, Edmonton, AB T6G 2G8, Canada
[d] Faculty of Pharmacy and Pharmaceutical Sciences, University of Alberta, Edmonton, AB T6G 2G8, Canada

ARTICLE INFO

Article history:
Received 1 November 2012
Accepted 2 January 2013
Available online 23 January 2013

Keywords:
siRNA
Polyethylenimine
Lipid
Molecular dynamics
Polyplex
Gene delivery

ABSTRACT

Polycations have been explored as non-viral carriers for effective delivery of small interfering RNA (siRNA). Modifying polycations such as polyethylenimine (PEI) with lipid substitution was found to improve the siRNA delivery efficiency of polycationic carriers. However, the role of such lipid modification is not clear and remains to be probed at the atomistic level. In this work, we elucidate the role of lipid modification through a series of all-atom molecular dynamics simulations on siRNA complexation mediated by a native PEI and four analogous obtained by different lipid modifications. The lipid modification does not affect PEI's capability of neutralizing the siRNA charge, neither does it affect the polyion bridging which plays an important role in siRNA complexation. Significant linkages among the lipid modified PEIs via association of lipid side-groups are observed and this results in more stable and compact PEI/siRNA polyplexes. The lipid associations between short lipids form and break frequently while the lipid associations between long lipids are more stable. For PEIs modified with short lipids, increasing the lipid substitution level results in more compact and stable siRNA structure. For PEIs modified with long lipids, increasing the lipid substitution does not change the amount of PEI linkage via lipid association, and has a reverse effect on compacting siRNA structure due to increased steric hindrance brought by the lipid association on individual PEIs. The simulation results generally correlate well with experimental data and suggest a framework of designing and systematic evaluation of polycation-based siRNA carriers using molecular dynamics simulations.

© 2013 Elsevier Ltd. All rights reserved.

1. Introduction

RNA interference (RNAi) via small interfering RNA (siRNA) is a promising therapeutic strategy which have attracted intense attention during the past decade [1,2]. Protective carriers are needed to deliver siRNA to the target site (cytosol) since siRNA is rapidly degraded by nucleases in the biological environment in its native form. siRNA itself cannot permeate cell membrane on its own, given the anionic charge of the cell membrane and the siRNA itself. Delivering siRNA into cells in an effective way is a major impediment for its successful therapeutic applications. Polycationic carriers, such as polyethylenimine (PEI) [3,4], have evolved into a major approach for siRNA delivery with the advantage of being readily modified with other functional groups, making it possible to tailor their properties for different applications [5]. In addition, polycationic carriers do not arouse the safety concerns associated with viral carriers [6,7]. High molecular weight (HMW, ~25 kDa) PEIs is one class of effective carriers for siRNA delivery and often considered as 'gold standard' in non-viral gene delivery, however, the high toxicity and limited biodegradability prohibit their clinical use. Low molecular weight (LMW, <2 kDa) PEIs display acceptable toxicity but cannot effectively deliver siRNA into cells. Modifying polycations with lipophilic and hydrophobic moieties was found to improve the performance of polycation-based gene delivery carriers [5,8]. Modifying poly-L-lysine (PLL) with a lipid, for example, greatly enhanced the siRNA delivery efficiency with increased cellular uptake and better protection from siRNA degradation [9,10]. Cationic carriers containing cholesterol were found to improve siRNA delivery through an enhanced interaction with cell membrane [11]. The impact of different lipid substitution on the assembly and delivery of siRNA by 2 kDa PEI was investigated, and lipid substitution was found to significantly increase the cellular uptake and lead to effective gene knockdown with minimal cytotoxicities [12]. It was also found that

* Corresponding author. 4-9 Mechanical Engineering Building, Department of Mechanical Engineering, University of Alberta, Edmonton, AB T6G 2G8, Canada. Tel.: +1 780 492 5467; fax: +1 780 492 2200.
E-mail address: tian.tang@ualberta.ca (T. Tang).

0142-9612/$ – see front matter © 2013 Elsevier Ltd. All rights reserved.
http://dx.doi.org/10.1016/j.biomaterials.2013.01.011

not all the lipid modifications were beneficial and the performance of modified PEIs depended on the nature of the substituted lipids and the level of substitution [12]. Despite the experimental evidence for the beneficial effects of the lipid modifications, the molecular mechanism behind the beneficial effects is not clear, and remains to be probed.

Computer simulations especially molecular dynamics (MD) simulations are playing an increasingly important role in studying nucleic acid complexation with carriers. Recent MD simulation studies provided insight into the self-assembly process and structure-binding relationship of siRNA with dendrimers [13–20]. They demonstrated the validity of using MD simulations to study the interaction between siRNA and supramolecular carriers. For example, the radius of gyration of the dendrimer calculated from the simulation was consistent with the SAXS measured value [20]. However, these simulation studies only investigated the interaction of carriers with a single siRNA molecule, while in practical systems, the carriers are often interacting with multiple siRNA molecules to condense the siRNAs into nanoparticles. Simulations involving multiple siRNA molecules will provide a more realistic insight on the role of carriers in siRNA complexation process.

In order to elucidate the mechanisms of PEI mediated siRNA complexation and condensation, we performed a series of large scale all-atom MD simulations with four siRNA molecules. We specially focused on the role of lipid substitution in siRNA binding and condensation. A branched 2 kDa PEI was adopted as the native PEI and four PEIs modified with caprylic acid (CA) and linoleic acid (LA) at two substitution levels were adopted as the lipid modified PEIs. These conjugates were chosen due to the availability of extensive experimental data on their siRNA delivery capabilities. Our study aims to shed light on the structure–function relationship by analyzing the structures of PEI/siRNA polyplexes and correlating them with experimental data.

2. Methods

2.1. Simulated systems and procedure

The siRNA simulated in this study has the following sequence: sense: 5′-CAGAAAGCUUAGUACCAAATT-3′, antisense: 5′-UUUGGUACUAAGCUUUCUGTC-3′, which was used extensively to silence P-glycoprotein [9,10,12]. It is composed of 42 nucleotides carrying a total charge of −40 in the fully de-protonated state. The initial structure of the siRNA was built to be a canonical A form using the AMBER NAB tool [21]. The native PEI simulated is a branched PEI which consists of 43 amine groups (primary, secondary and tertiary) and has a molecular mass of 1874 Da [22]. Four lipid-modified PEIs were adopted and referred to as: P_1CA, PEI with one caprylic acid (CA); P_3CA, PEI with three CAs; P_1LA, PEI with one linoleic acid (LA); and P_3LA, PEI with three LAs. These levels of substitution are in the practical range where functional differences were observed from the native PEI in siRNA delivery [12]. To facilitate the discussion herein, we generally refer to both the native PEI and lipid modified PEIs as PEIs. The chemical structures and protonation sites of the five PEIs are shown in Fig. 1. For the native PEI, 20 amine groups (marked by '+' and #1, #2, #3 in Fig. 1) were chosen to be protonated, corresponding to a protonation ratio of 47% as recently found experimentally at pH = 6 [23]. The protonation sites were assigned to only the primary and secondary amines, and were arranged as uniformly as possible to minimize thermodynamic interactions between the protonated amines. For P_1CA and P_1LA, the corresponding lipid is grafted on the native PEI at site #1 as shown in Fig. 1. Similarly, for P_3CA and P_3LA, three lipids are grafted on

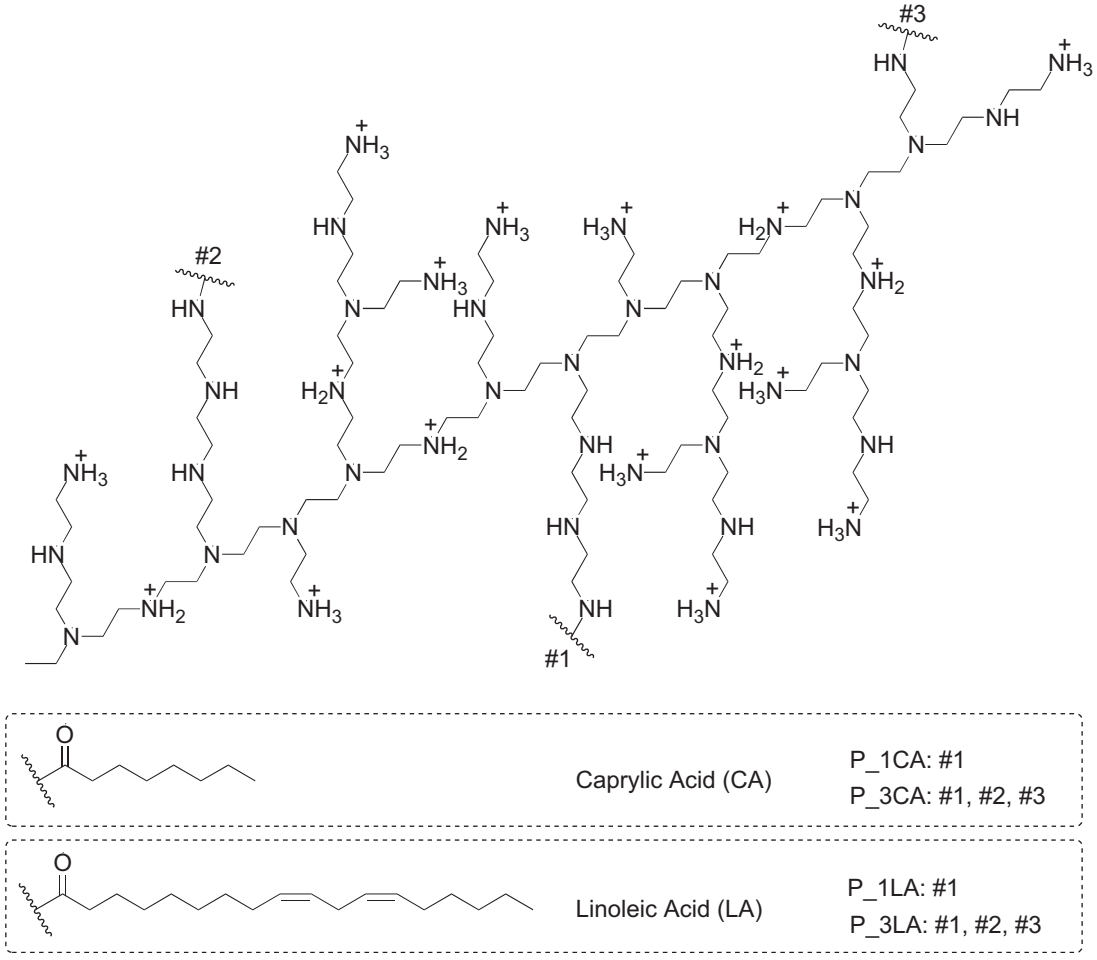

Fig. 1. Molecular structure, protonation sites and lipid substitution sites of the five PEIs studied.

Table 1
Information of the five single PEI systems simulated in this study.

System name	Charge of the PEI	Number of atoms	Size of simulation box (Å^3)	Number of Na^+/Cl^-	Simulation time restrained + free (ns)
P2k	20	37,160	58 × 69 × 92	0/20	0.2 + 50
P_1CA	19	20,096	58 × 58 × 58	0/19	0.2 + 40
P_3CA	17	20,123	58 × 58 × 58	0/17	0.2 + 40
P_1LA	19	20,215	58 × 58 × 58	0/19	0.2 + 40
P_3LA	17	20,042	58 × 58 × 58	0/17	0.2 + 40

the native PEI at sites #1, #2, #3 as shown in Fig. 1. The initial structures of the PEIs were built in VMD [24] and then energetically minimized in NAMD [25] to obtain the initial PEI structures for the subsequent MD simultations. Five initial MD simulations were first performed for the PEIs, each of which contained one PEI with explicit water and a number of Cl^- ions to neutralize the systems (Table 1). The structure of each PEI at the end of the simulation was adopted as the initial configuration for PEIs in the simulations of PEI mediated siRNA complexation.

Five systems were then simulated to study the PEI mediated siRNA complexation, each of which contains 4 siRNAs and 18 PEIs corresponding to a PEI/siRNA N/P charge ratio of ~2. For each system, appropriate amount of Na^+ and Cl^- ions were added to simulate the salt concentration of 154 mM at physiological levels. Detailed information of the five systems is summarized in Table 2. In this article, each system will be referred to by its name in the first column of Table 2. In constructing the initial configurations for each of the five systems, the axes of the four siRNAs were aligned to be parallel to one another and positioned on the four corners of a square with 35 Å side length. The principal axes of the PEIs were initially aligned parallel to the siRNA axes, and the center of mass (COM) of each PEI was positioned at 25 Å away from the axis of its neighboring siRNA(s). Detailed arrangement of the initial configurations is illustrated in Fig. 2.

2.2. Simulation details

A CHARMM format force field was developed and validated [26] for PEI based on the CHARMM General Force Field [27], and CHARMM 27 force field [28,29] was used for all other molecules. All simulations were performed using the MD package NAMD [25]. TIP3P water model [30], periodic boundary condition, full electrostatics with particle-mesh Ewald method [31], cutoff distance 10 Å for van der Waals interactions and electrostatics pairwise calculations, SHAKE algorithm [32] to constrain all bonds containing hydrogens, and a time step of 2 fs were used for all the simulations.

For each system, the PEI/siRNA molecule(s) were first solvated into a cubic water box. Ions were then added into the water box by randomly replacing equivalent amount of water molecules using VMD [24]. During each simulation, the system was first minimized for 5000 steps, then heated from 0 K to 300 K in 20 ps with 10 kcal/(mol × Å^2) harmonic restraint on the non-hydrogen atoms of the solute. The restraint was kept on for 200 ps for the single PEI systems or 10 ns for the PEI/siRNA complex systems at 300 K and 1 bar to relax the ions around the solutes. The restraint was then removed and NPT ensemble simulation was performed for 40–50 ns for the single PEI systems or 200 ns for the PEI/siRNA complex systems. VMD [24] was used for visualization and trajectories analysis.

3. Results and discussion

3.1. Dynamics of siRNA complexation

Fig. 2 shows snapshots of the initial and final configurations for the five polyplexes, where the lipid moieties on the PEIs in Fig. 2(b–d) are represented by spheres. For all five systems, the four siRNAs are centrally sequestered in the polyplexes formed with the PEIs at the end of the simulations. In systems 4R-18P, 4R-18P_1CA and 4R-18P_1LA, several PEIs are not attached to the formed polyplexes and exist freely in solution, unlike the polyplexes formed with PEIs containing higher lipid content, P_3CA and P_3LA.

To investigate the dynamics of PEIs binding during the complexation process, we plotted the numbers of PEIs bound to siRNAs as a function of time (Fig. 3). Here we define a PEI to be bound to siRNAs if it has at least one N within 4 Å of any siRNA N/O atoms. For all five systems, the numbers of PEIs bound to the siRNAs rise quickly to ~16 during the first 10 ns of the simulations. The curves display significant fluctuation from 10 to 50 ns, after which the fluctuations diminish to some degree. At the late stage of the simulations, the bound PEIs stabilize at around 16, 16, 18, 15, 16 for systems 4R-18P, 4R-18P_1CA, 4R-18P_3CA, 4R-18P_1LA and 4R-18P_3LA, respectively. Since a PEI carries a positive charge of 17–20 and the four siRNAs carry a negative charge of −160, all the five polyplexes formed are positively charged, which is consistent with the experimental observations [12]. Comparison between the data in Fig. 3 and the final configurations of the polyplexes suggest that some lipid modified PEI molecules involved in a polyplex are not directly bound to the siRNAs. These PEIs in fact attach to the polyplex through lipid association with other PEIs, which is an important mechanism for siRNA complexation by lipid modified PEIs and will be discussed in detail later.

Macromolecular association in aqueous environments usually results in the release of water molecules previously adhering to surfaces of the macromolecules. In our work, monitoring the number of the water molecules on the PEIs/siRNAs surface allows us to monitor the complexation process and to gauge whether dynamic equilibrium has been reached. Since the water molecules on the macromolecular surfaces are less mobile than those in the free bulk state, such release is an entropically favorable process with a free energy reduction of up to 2 kcal/mol at 300 K [33]. Therefore, the number of water molecules released during the macromolecule association allows us to assess the entropic gain upon macromolecular binding. Fig. 4 shows the numbers of water molecules in the hydration shell of the PEIs/siRNAs (within 3 Å from the molecules) as a function of simulation time. For all five systems, the number of water molecules in the hydration shell drop quickly during the first 50 ns, indicating that as the polyplexes form, a large number of water molecules were displaced from the PEI and siRNA surfaces into the bulk during this period. The curves start to level off after 100 ns, indicating dynamic equilibriums have been reached. Table 3 summarizes the number of water molecules released from the hydration shell of the solutes at the end of the simulation time. Detailed information on this calculation is given in Supplementary Data. The released water molecules are higher for the systems with lipid-modified PEIs than for system 4R-18P with native PEIs. With more lipid substitution on PEIs, more water molecules are released: 4R-18P_1CA (1588) vs. 4R-18P_3CA (1910) and 4R-18P_1LA (1861) vs. 4R-18P_3LA (2054). The longer alkyl chain in P_1LA and P_3LA leads to more water molecules being released, as compared with the systems with the same level of CA substitution. The lipids are expected to associate in aqueous solution to reduce their solvent

Table 2
Information of the five PEI/siRNA systems simulated in this study.

System name	Lipid no./type on each PEI	Charge ratio siRNA/PEI	Number of atoms	Size of simulation box (Å^3)	Number of Na^+/Cl^-	Simulation time restrained + free (ns)
4R-18P	None	160/360	157,456	115 × 115 × 115	136/336	10 + 200
4R-18P_1CA	1 CA	160/342	157,210	115 × 115 × 115	136/318	10 + 200
4R-18P_3CA	3 CA	160/306	156,817	115 × 115 × 115	136/282	10 + 200
4R-18P_1LA	1 LA	160/342	156,787	115 × 115 × 115	136/318	10 + 200
4R-18P_3LA	3 LA	160/306	156,496	115 × 115 × 115	136/282	10 + 200

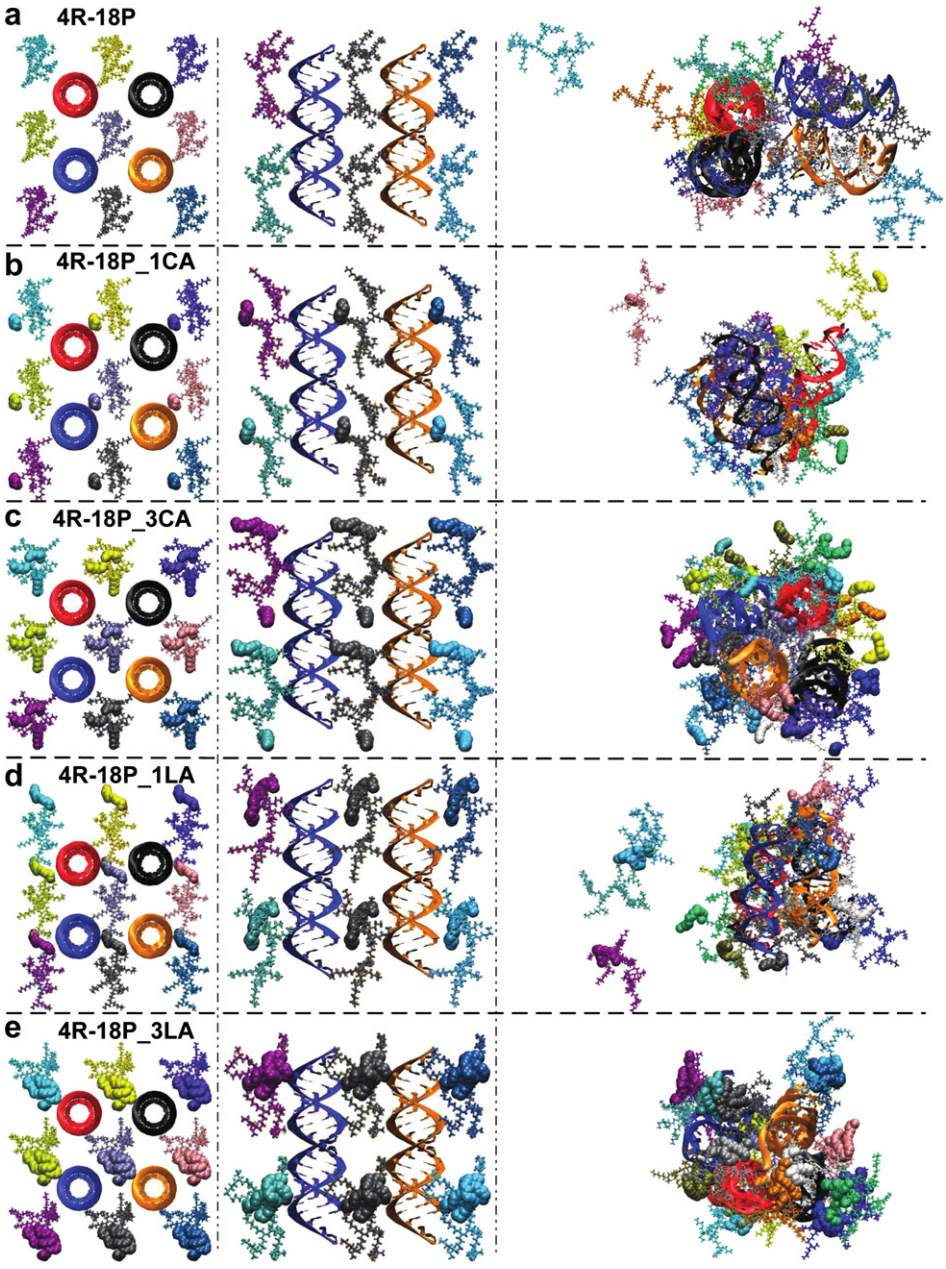

Fig. 2. Initial (left panel – axis view, central panel – side view) and final configurations (right panel) of the five PEI/siRNA systems: (a) 4R-18P, (b) 4R-18P_1CA, (c) 4R-18P_3CA, (d) 4R-18P_1LA, (e) 4R-18P_3LA. Different PEIs and siRNAs are represented in different colors; the lipid moieties on the PEIs are represented by spheres; water and ions are removed for clarity.

accessible surface. The larger amount of water release for systems with lipid modified PEIs is likely to reflect water released from the lipid association. We will address the lipid association later in this work.

3.2. Polyion bridging and siRNA charge neutralization

We previously identified two main mechanisms for native PEI mediated DNA complexation [34]: polyion bridging (i.e., a polycation spanning across multiple DNA segments simultaneously; see detailed definition in Supplementary Data) and DNA charge neutralization. As expected, we found that polyion bridging also plays an important role in PEI mediated siRNA complexation. Specially, for systems 4R-18P, 4R-18P_1CA, 4R-18P_3CA, 4R-18P_1LA and 4R-18P_3LA, 7, 7, 8, 9, 8 PEIs, respectively, participated in bridging two or three siRNAs for longer than 50% of the simulation time (see Figs. S1–S5 in Supplementary Data). These close numbers indicate that lipid substitution does not affect the polyion bridging behavior of the PEIs.

To investigate how the five different PEIs neutralize the siRNA charges, we plotted the cumulative distributions, with respect to the siRNA C1′ atoms, of PEI N+, Na^+, Cl^- and the total charge of PEI/salt ions, averaged over the last 80 ns of the simulations (Fig. 5). The C1′ atoms are on the sugar rings of the siRNAs, located inside the siRNA helix at a distance of ~5 Å from the surface of siRNA defined by the phosphorus atoms. In each subfigure of Fig. 5, the dashed black line indicates the −160 charge of the four siRNAs, and the blue solid curve is the total charge of PEI and salt ions within given

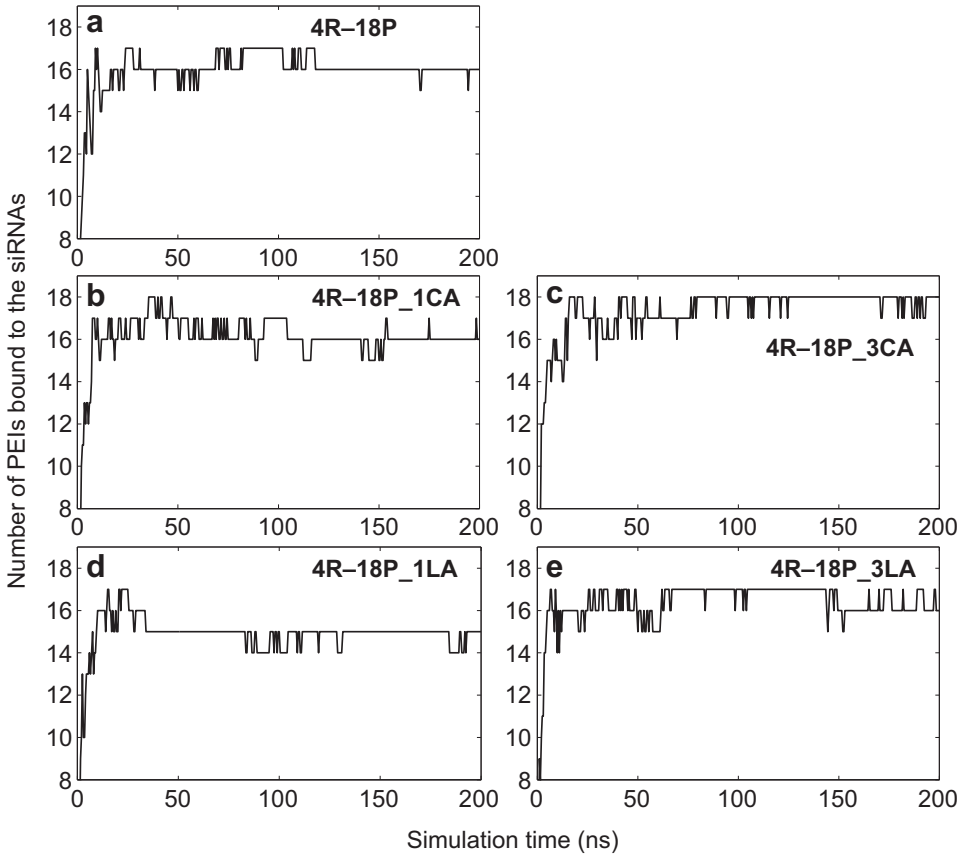

Fig. 3. Number of PEI molecules bound to the siRNAs as a function of simulation time. (a) 4R-18P, (b) 4R-18P_1CA, (c) 4R-18P_3CA, (d) 4R-18P_1LA, (e) 4R-18P_3LA.

distance to their nearest siRNA C1′ atoms. The four siRNA are 100% neutralized by the PEIs and salt ions at the distance where the black dashed line and blue curve intersect. It can be seen that the curves for the five systems share a similar characteristic. For all the systems, the PEIs/ions neutralize the siRNA at a distance of ~8 Å from the siRNA C1′ atoms. Within 8 Å, it can be seen that the distribution of Cl^- and Na^+ ions is minimal and almost identical, and the curves for the net charge of PEI/ions basically overlaps with the curves for the PEI charge. Therefore, we conclude that the PEIs contribute dominantly in neutralizing the siRNA within the 8 Å of the siRNA C1′ atoms. Being capable of neutralizing the siRNAs at such a short distance is a major mechanism for PEI mediated siRNA complexation. At distances beyond the intersection of the black line and the blue curve, the PEI and ion charges exceed the siRNA charges, i.e., the siRNAs are over-neutralized at such distances. The five systems have a similar extent of maximum over-neutralization of ~25 charges at ~18 Å from the siRNA C1′ atoms. The similar neutralizing characteristic for the five PEIs demonstrates that the lipid substitution on PEIs does not affect their capability of neutralizing the siRNA molecules. In Fig. S6 of Supplementary Data, we plotted the charge neutralization curves based on four different time windows at the late stage of the simulations as an evidence for convergence of the simulation trajectories.

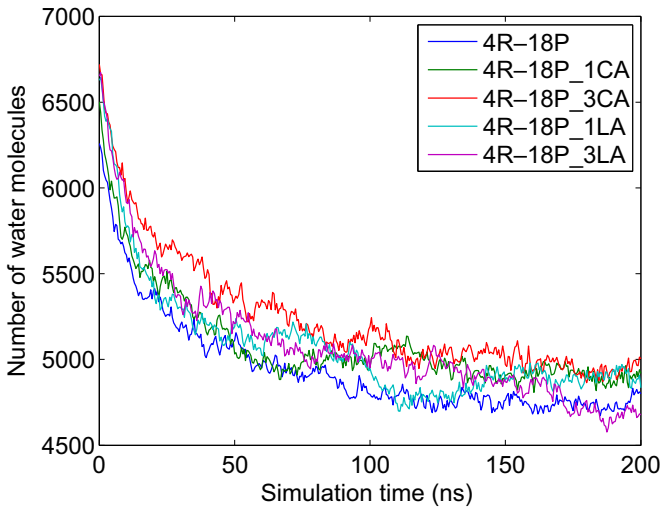

Fig. 4. Number of water molecules in the hydration shell (within 3 Å of the siRNAs and PEIs) as a function of simulation time.

3.3. Lipid association

Visual examination of the final configurations in Fig. 2(b–e) shows that some lipid tails from different PEIs are associated at the end of the simulation. The much larger amount of water release with lipid modified PEIs was also indicative of significant association among the lipids. To quantify the lipid association among

Table 3
Number of water molecules released from the solute during the complexation process.

System	4R-18P	4R-18P_1CA	4R-18P_3CA	4R-18P_1LA	4R-18P_3LA
No. of waters	1577	1588	1910	1861	2054

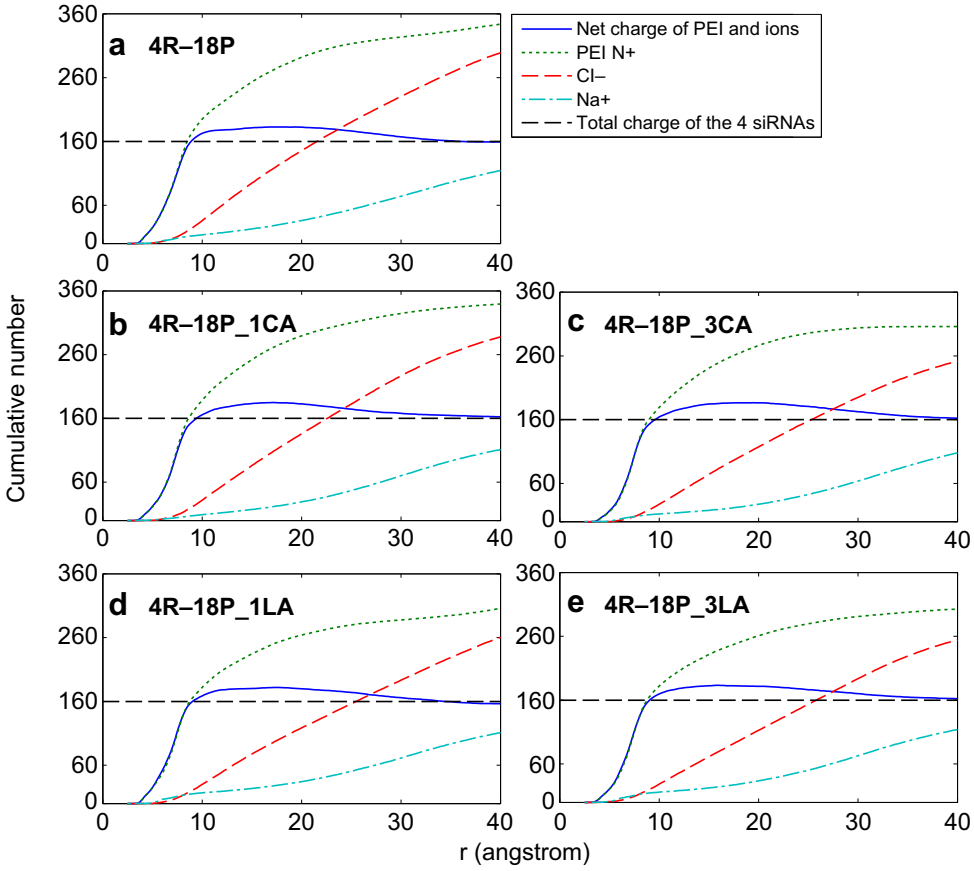

Fig. 5. Cumulative numbers of protonated PEI Ns, Na^+, Cl^-, and net charge of PEI/Na^+/Cl^- as a function of the distance from any RNA C1′ atom (averaged over the last 80 ns of each simulation). The total charge of the four siRNAs is plotted by a straight dashed black lines as reference in each subfigure. (a) 4R-18P, (b) 4R-18P_1CA, (c) 4R-18P_3CA, (d) 4R-18P_1LA, (e) 4R-18P_3LA.

different PEIs, in Fig. 6, we tabulated the number of pairs of lipid carbons that are closer than 5 Å between each pair of PEIs, averaged over the last 40 ns of the simulations. The numbers on the top and right of each subfigure are the PEI indices. The 18 PEIs in each system results in 153 possible pairing of PEIs, corresponding to 153 cells in each subfigure of Fig. 6. A CA lipid has 8 carbons so that one pair of P_1CA would have 64 pairing of carbons. Similarly, for 4R-18P_3CA, 4R-18P_1LA and 4R-18P_3LA, all possible pairing of carbons would be 576, 324 and 2916, respectively. Among these possible carbon pairs, the number of pairs within 5 Å are counted and given in the cell corresponding to this pair of PEIs. The cells are left empty where no carbon pair was found to be within 5 Å. For examples, number 9 on the top left of Fig. 6(a) means that out of the 64 pairs of carbons between PEI 1 and PEI 3 in system 4D-18R_1CA, 9 pairs are separated by 5 Å or less; number 169 on the bottom of Fig. 6(d) means that out of the 2916 pairs of carbons between PEI 15 and PEI 16 in system 4D-18R_3LA, 169 pairs are separated by 5 Å or less. We choose 5 Å as the criterion because this is the closest carbon–carbon distance within which the free energy for the association of two alkane molecules is negative, indicating that their association is energetically favorable [35]. The situation of at least one pair of carbon being closer than 5 Å apart is considered to represent linked PEI molecules through lipid association. Only two pairs of PEIs are linked in system 4D-18R_1CA (Fig. 6(a)). For system 4D-18R_3CA with increased level of substitution, the intensity of lipid association is dramatically increased, with 11 pairs of PEIs linked (Fig. 6(b)). Between each of these 11 pairs of PEIs, 5.7 pairs of lipid carbons (on average) are closer than 5 Å apart. Systems 4D-18R_1LA and 4D-18R_3LA have 6 and 8 pairs of PEIs linked, respectively, with the average numbers of lipid carbon pairs between each pair of linked PEIs being 35 and 107. There are three PEIs mutually linked in systems 4D-18R_1LA and 4D-18R_3LA, which are marked by gray cells in Fig. 6(c, d). When the level of lipid substitution increases, the number of linked PEIs through lipid association do not increase as dramatically for LA substituted PEIs as that for CA substituted PEIs, however, the average number of lipid carbon pairs between each pair of linked PEIs increases by approximately three times for the longer lipid. For systems 4D-18R_1CA and 4D-18R_1LA with one lipid substitution per PEI, with longer lipid chain, the intensity of lipid association increased dramatically in terms of both number of linked PEIs and average number of lipid carbon pairs between each pair of linked PEIs. For systems 4D-18R_3CA and 4D-18R_3LA with three lipid substitution per PEI, with longer lipid chain, the number of linked PEIs actually decrease from 11 to 8, however, the average number of lipid carbon pairs between each pair of linked PEIs is almost 19 times as high for 4D-18R_3LA.

To investigate how the lipid associations evolve during the simulations, we plotted the number of lipid carbon pairs that are closer than 5 Å apart between certain pairs of PEIs as a function of simulation time in Fig. 7. Only those pairs of PEIs that have lipid association during the last 40 ns as marked in Fig. 6 are considered. For 4D-18R_1CA (Fig. 7(a)), the curves undergo rapid fluctuation between 0 and 20, indicating that the lipid associations between the two pairs of PEIs are highly unstable. Increasing the lipid substitution level from 1 CA to 3 CA per PEI does not change the

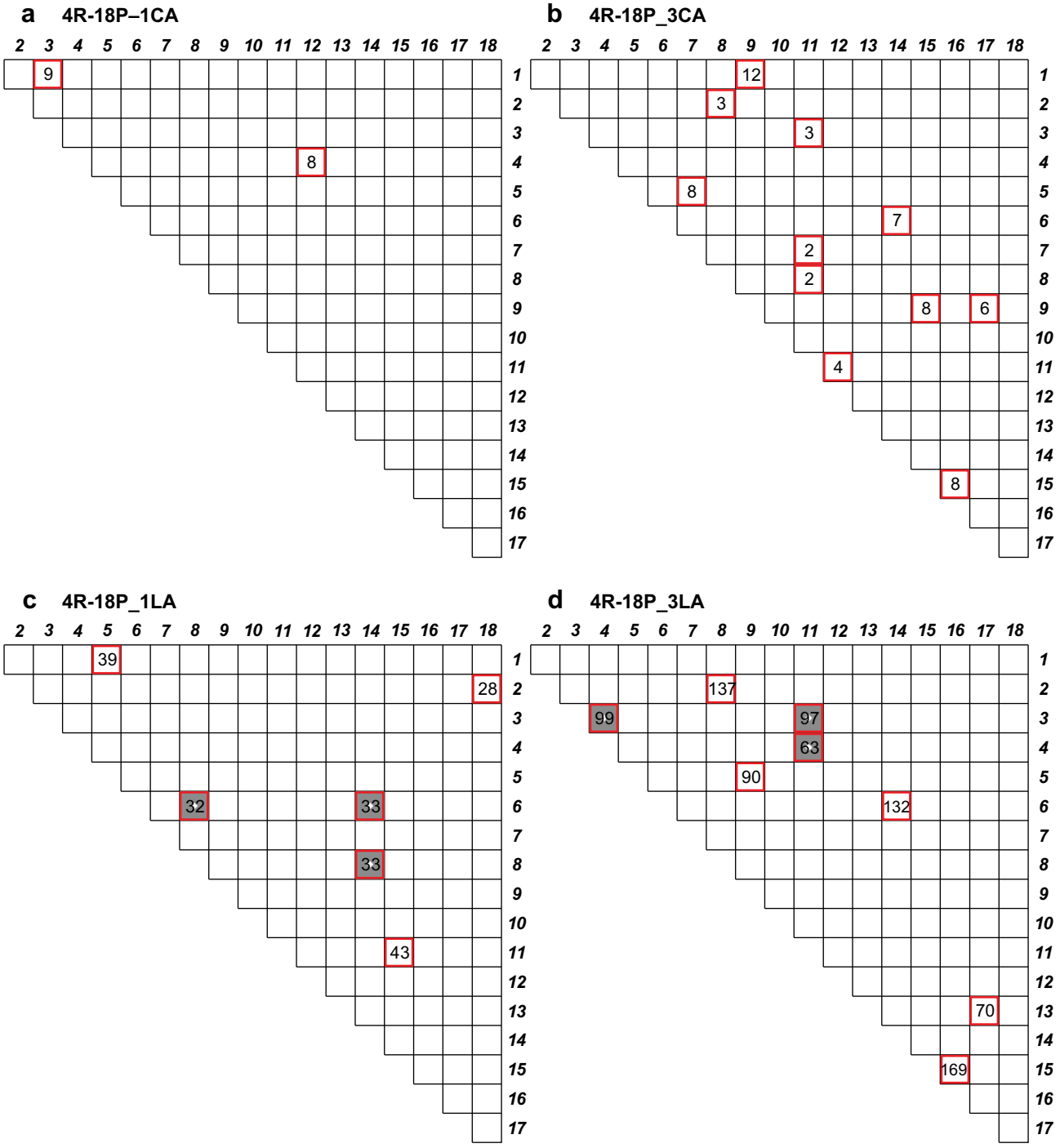

Fig. 6. Number of pairs of lipid carbons that are closer than 5 Å apart between each pair of PEIs, averaged over the last 40 ns of the simulations in (a) 4R-18P_1CA, (b) 4R-18P_3CA, (c) 4R-18P_1LA, (d) 4R-18P_3LA. The numbers on the top and right of each subfigure are PEI indices. Only the non-zero numbers are shown and marked with red squares. The PEIs involved in the same association are marked by gray cells in (c, d). (For interpretation of the references to color in this figure legend, the reader is referred to the web version of this article.)

unstable nature of the lipid associations for the 11 pairs of PEIs in 4D-18R_3CA (Fig. 7(b)). The associations fluctuate rapidly between 0 and 40, for example, the lipid association between PEIs 11 and 12 breaks for ~20 times during the 200 ns simulation time. For 4D-18R_1LA with long LA lipid (Fig. 7(c)), both the magnitude of fluctuation and the frequency of breakage of lipid associations are reduced. Five lipid associations (PEIs 1-5, 6-8, 6-14, 8-14, 11-15) out of the six still break for several times during the simulations. Unlike for CA, increasing the LA substitution level stabilizes the lipid association (Fig. 7(d)), evidenced by that the eight lipid associations never break apart once they are formed in the simulations.

For PEIs with 3 CA or 3 LA substituents, the three lipids within one PEI could associate and this can make the PEI molecule more rigid. Table 4 tabulates the lipid association status among the three lipids on individual PEIs in systems 4D-18R_3CA and 4D-18R_3LA. If none of the three lipids on a PEI is associated, it is marked with 'N'; if the three lipids are mutually associated, it is marked with 'A'; otherwise, the three lipids are partially associated and marked with

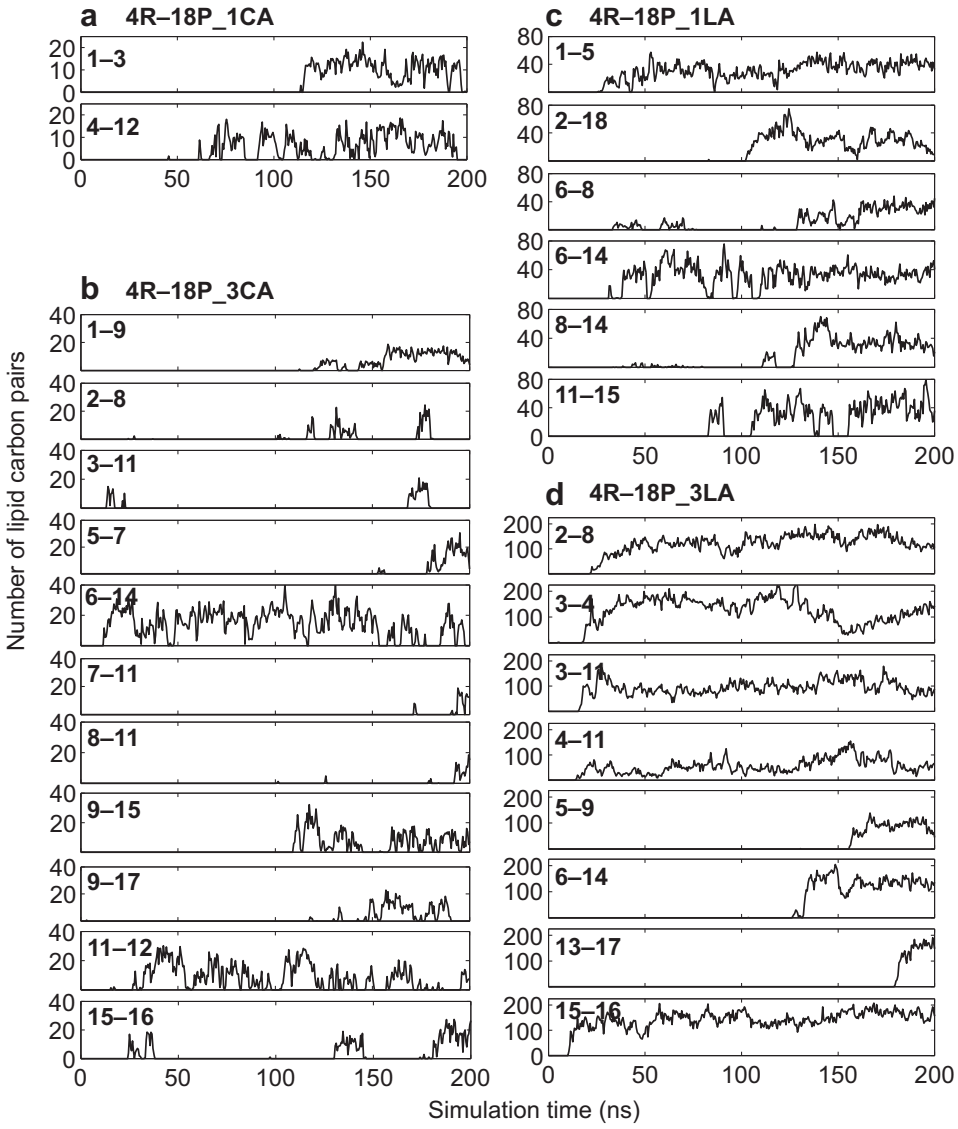

Fig. 7. Dynamics of lipid association: Number of pairs of lipid carbons that are closer than 5 Å between certain pairs of PEIs as a function of simulation time in (a) 4R-18P_1CA, (b) 4R-18P_3CA, (c) 4R-18P_1LA, (d) 4R-18P_3LA. The two numbers in each subfigure are the indices of the pair of PEIs.

'P'. For all the 18 PEIs in 4D-18R_3LA, the three lipids on each PEI are mutually associated, while for 4D-18R_3CA only two PEIs have their three lipids mutually associated. Ten PEIs in 4D-18R_3CA have the three lipids partially associated and six PEIs have no self lipid association. The universal lipid association on individual P_3LAs in system 4D-18R_3LA could cause the P_3LAs possess more rigidity and hence manifest a mere profound steric effect when binding to siRNA. Such effect can be seen from the compactness of the siRNAs as demonstrated below.

3.4. Compactness of the siRNAs

To gauge the compactness of the siRNA molecules in the polyplexes and their stability, we plotted the radii of gyration R_g of the four siRNA molecules as a function of simulation time in each system (Fig. 8). For a given polyplex, a higher value of R_g is an indicator of more loosely arranged siRNA molecules in the polyplex. For all the five systems, the R_g curves follow a generally decreasing trend during the first 50 ns of the simulations, indicating the formation of the siRNA polyplexes while the siRNA molecules are moving closer. The R_g values fluctuate from 50 ns to 200 ns. During the last 80 ns of the simulations, the average R_g of the four siRNAs are 31.0 Å, 29.1 Å, 27.9 Å, 27.0 Å and 28.0 Å, and the variance of the R_g are 0.19 Å, 0.08 Å, 0.05 Å, 0.05 Å and 0.11 Å for systems 4R-18P, 4R-18P_1CA, 4R-18P_3CA, 4R-18P_1LA and 4R-18P_3LA, respectively. The 4R-18P has the most loose and least stable siRNA structure among the five polyplexes indicated by the largest R_g and largest variance. This indicates that the lipid modification compacts

Table 4
Lipid association among the three lipids on individual PEIs in systems 4R-18P_3CA and 4R-18P_3LA (N – none; P – partially; A – all).

PEI index	1	2	3	4	5	6	7	8	9	10	11	12	13	14	15	16	17	18
4R-18P_3CA	N	P	N	P	P	P	P	N	N	P	N	P	A	P	N	P	P	A
4R-18P_3LA	A	A	A	A	A	A	A	A	A	A	A	A	A	A	A	A	A	A

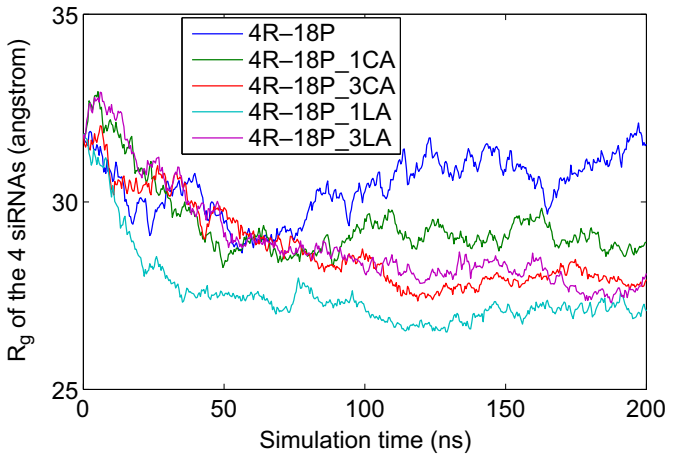

Fig. 8. Radius of gyration of the four siRNAs in each system as a function of simulation time.

and stabilizes the siRNA polyplexes. The siRNAs in system 4R-18P_1CA have a larger and more fluctuating R_g compared to the siRNAs in 4R-18P_3CA. This is expected as the more lipid substitution per PEI, the more profoundly the effects of the lipid substitution manifest. However, the siRNAs in system 4R-18P_3LA have a larger R_g compared to the siRNAs in 4R-18P_1LA with less lipid substitution. It seems therefore that higher lipid substitution level does not necessarily lead to more compact siRNA structure. This can be explained by the fact that the association of the three LA lipids on individual PEIs generates a significant steric hindrance for condensing the siRNAs.

3.5. Location of cationic and lipophilic moieties of PEIs

Although the size and charge of carrier/siRNA polyplexes are routinely assessed in experiments, the structural details especially the location of the lipophilic moieties in the polyplexes have not been investigated experimentally [8]. To assess the location of cationic and lipophilic moieties of the PEIs relative to the siRNAs, in Fig. 9 we plotted the cumulative percentage (left panel) and radius distribution function (right panel) of the PEI Ns and lipid carbons as a function of distance from any siRNA N/O atom, averaged over the last 80 ns of the simulation. Taking the PEI Ns for example, the cumulative percentage at a given distance r is the percentage of all the PEI Ns within a distance r from any siRNA N/O atoms. For all the five systems, the cumulative percentage curves for the PEI Ns rise quickly from 0% at 2.5 Å to ~40% at 5 Å, and to ~80% at 15 Å. The curves for lipid carbons rise from 3 Å (0%) following a similar trend as the curves for PEI Ns, but the lipid carbon curves generally right shift by 1–2 Å of the PEI Ns curves. This clearly shows that the lipophilic moieties are located further away from the siRNAs than the cationic moieties. The corresponding subfigures in the right panel of Fig. 9 show the detailed distribution of the PEI Ns and lipid carbons with respect to the siRNA N/O atoms. The five systems have a similar pattern of PEI N distribution. There are two predominant peaks: one at ~2.5 Å and one at ~4.5 Å. The first peak corresponds to the expected distance for direct contact between the PEI amine groups and the siRNA N/O atoms through hydrogen bonding. The second peak corresponds to the distance for indirect interactions, such as hydrogen bonding mediated by one water molecule. Each of the two peaks corresponds to ~20% of the total PEI Ns. The similar pattern of PEI N distribution among the five systems demonstrates that lipid modification does not seem to affect the interaction between the siRNAs and the cationic moieties of PEIs, which is also consistent with the similar neutralization capability the five different PEIs demonstrate. The lipid carbons have one predominant peak at ~4 Å, and this peak accounts for ~40% of the total lipid carbons for systems 4R-18P_1CA and 4R-18P_1LA, ~35% carbons for system 4R-18P_3CA and ~25% carbons for system 4R-18P_3LA. The less amount of lipid carbons at the vicinity of siRNAs in systems 4R-18P_3CA and 4R-18P_3LA is probably due to the lipid association among the three lipids on individual PEIs as discussed in the previous subsection, which makes the lipid tails more rigid and hence harder to comply with the siRNAs. For systems 4R-18P_1LA and 4R-18P_3LA with long LA lipids, there is a second peak for lipid carbons at ~8 Å, which is more pronounced for system 4R-18P_3LA. This can be explained by the fact that the long LA lipids are more probable to have their lipid carbons located further from the siRNAs due to their physical length. The lipid association among the three lipids on individual PEIs for system 4R-18P_3LA contributes to its more pronounced second peak because such association makes the lipid moieties harder to comply with the siRNAs as discussed above.

3.6. Implications

Molecular details of siRNA polyplexes derived from MD simulations are expected to be correlated to molecular features of siRNA complexes, as well as biologically relevant performance, such as cellular uptake, intracellular trafficking and functional silencing. Although one ultimately wishes to seek correlations with functional silencing effects, it is premature to undertake this at this stage since polyplex dissociation needs to take place for silencing and details of polyplex dissociation and interactions with endogenous solutes (such as the siRNA target mRNA) have not been attempted before with MD simulations. However, experimental studies on cellular uptake of polyplexes have been reported by our group prior to the MD simulations. Cellular uptake is a relatively simple, single-step process that should be more amenable for correlations with MD simulations (as compared to silencing).

The cellular uptake of siRNA polyplexes formed with CA- and LA-substituted PEIs is summarized in Fig. 10 [12,36,37]. Our experimental observations are derived from 3 different cell lines and we employed polymer:siRNA weight ratios of 2:1 or 8:1 in these studies (corresponding to (10–14):1 and (40–56):1 molar ratios, respectively, depending on the level and nature of lipid substitution). The simulations in this study were obtained by using a molar ratio of 4.5:1. First clear observation in all experimental uptake studies was the improved cellular delivery of siRNA with lipid substitutions as compared to native PEI. More stable nature of the polyplexes formed by lipid-substituted PEIs (given by R_g in this study) is confirmatory of general observations on the correlation between the complex stability and cellular uptake [38,39]. The presence of lipid moiety, which enhances the compatibility of polyplexes with lipid membrane, cannot be ruled out in this context. The siRNA uptake with CA-substituted PEIs is consistent in all three cell types employed, kidney tubule MDCK cells, breast cancer MDA-435 cells and breast cancer MDA-231 cells [12,36,37]; the uptake was correlated to CA substitution level under all conditions. MD simulation indicated low degree of lipid interactions with CA at low substitution and improving interactions with increasing substitution levels, resulting in higher stability of the polyplex (smaller fluctuation in R_g). Hence, increased stability of polyplexes with increasing CA levels revealed with MD simulations was consistent with the experimental uptake results. The siRNA uptake with the LA-substituted PEIs, on the other hand, was more complicated. At low substitution levels (e.g., 1 LA per PEI), LA substitution was more effective than CA for facilitating siRNA uptake. The MD simulations also indicated better interaction among LA lipids at such low

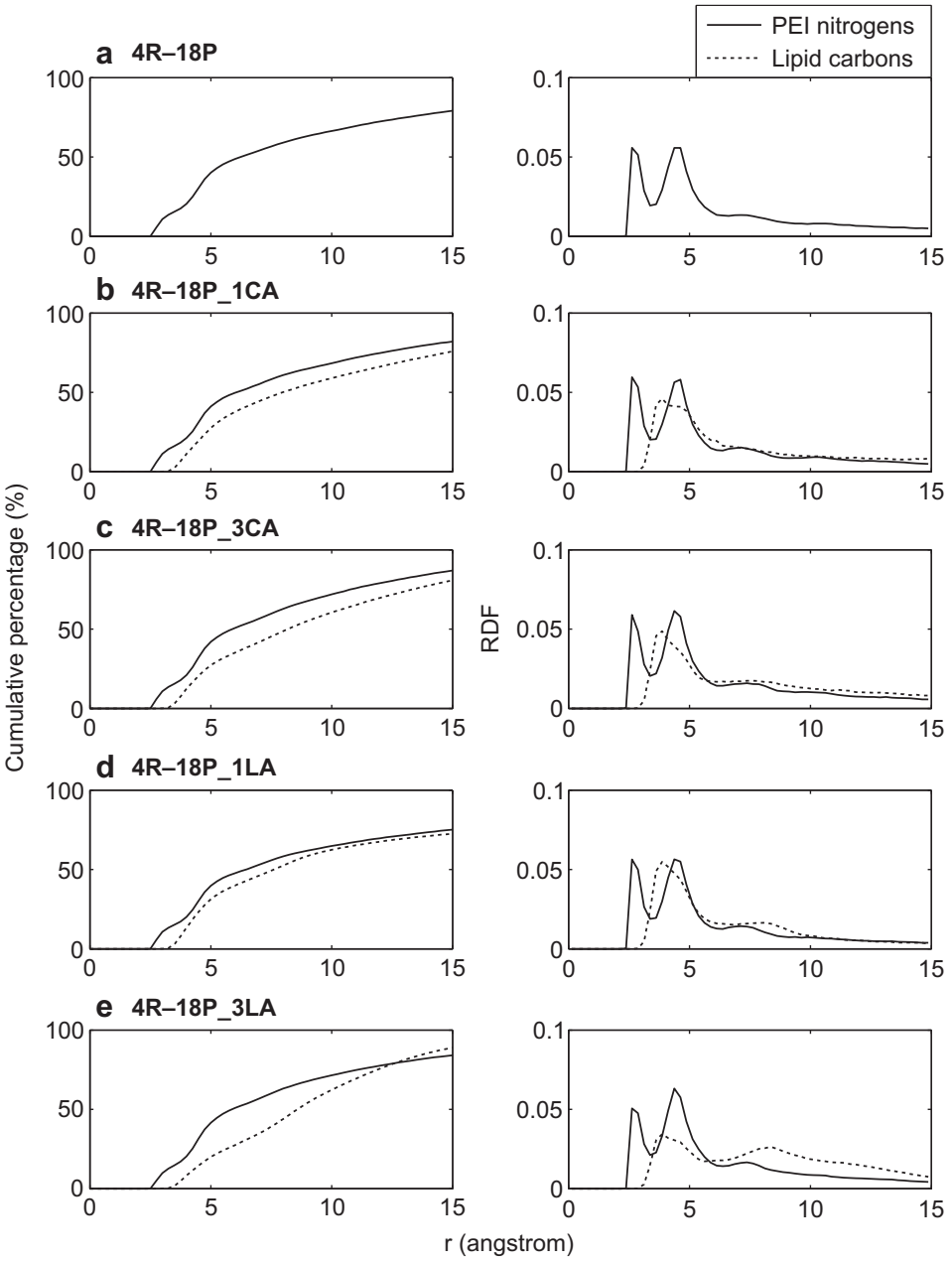

Fig. 9. Cumulative percentage (left panel) and radial distribution function (right panel) of the PEI Ns and lipid carbons as functions of the distance from the siRNA N/O atom in (a) 4R-18P, (b) 4R-18P_1CA, (c) 4R-18P_3CA, (d) 4R-18P_1LA, (e) 4R-18P_3LA.

substitution levels. Higher LA substitutions (e.g., 3 LAs per PEI) did not always lead to higher uptake in experimental studies, supportive of MD simulation results that indicated low level of substitutions to be sufficient to induce lipid–lipid interactions in the case of this longer lipid. The rigid PEI structure obtained with higher level of LA substitution could inhibit further siRNA binding, an observation noted on PAMAM dendrimers by Paven et al. [15]. The R_g values obtained for LA substituted PEI was not indicative of a correlation between the substitution level and the polyplex stability. The overall cellular uptake studies with this substituent also did not indicate a clear correlation between the uptake and substitution level. In that sense, the lack of strong correlations between LA substitution level and cellular uptake of siRNA was reflective of the effect of LA on calculated R_g values in this study.

One experimental observation not reproduced in this study is the higher charge (ζ-potential) of the polyplexes formed with lipid-substituted PEIs, as compared to polyplexes with native PEI. Better assembly of the polyplexes was evident with higher lipid substitution (see Fig. 2), which would have led to higher charges if all PEI molecules were equally charged. A limited numbers of PEIs were used in our simulations whereas the experimental studies usually employ higher PEI:siRNA ratios (as indicated above with the molar ratios). It is possible that more lipid-substituted PEIs could assemble to the polyplex with 4 siRNA and MD simulations might reveal such an effect when polyplexes are simulated with higher PEI:siRNA ratios. Secondly, the charges on PEI are considered fixed in this study, whereas a dynamic protonation state might change the overall charge of the polyplexes.

The peripheral lipids on the polyplexes can better protect the siRNAs from degrading nucleases, and also facilitate the interaction of the polyplexes with cell membranes and other hydrophobic biological entities on the delivery path. This lipid distribution and

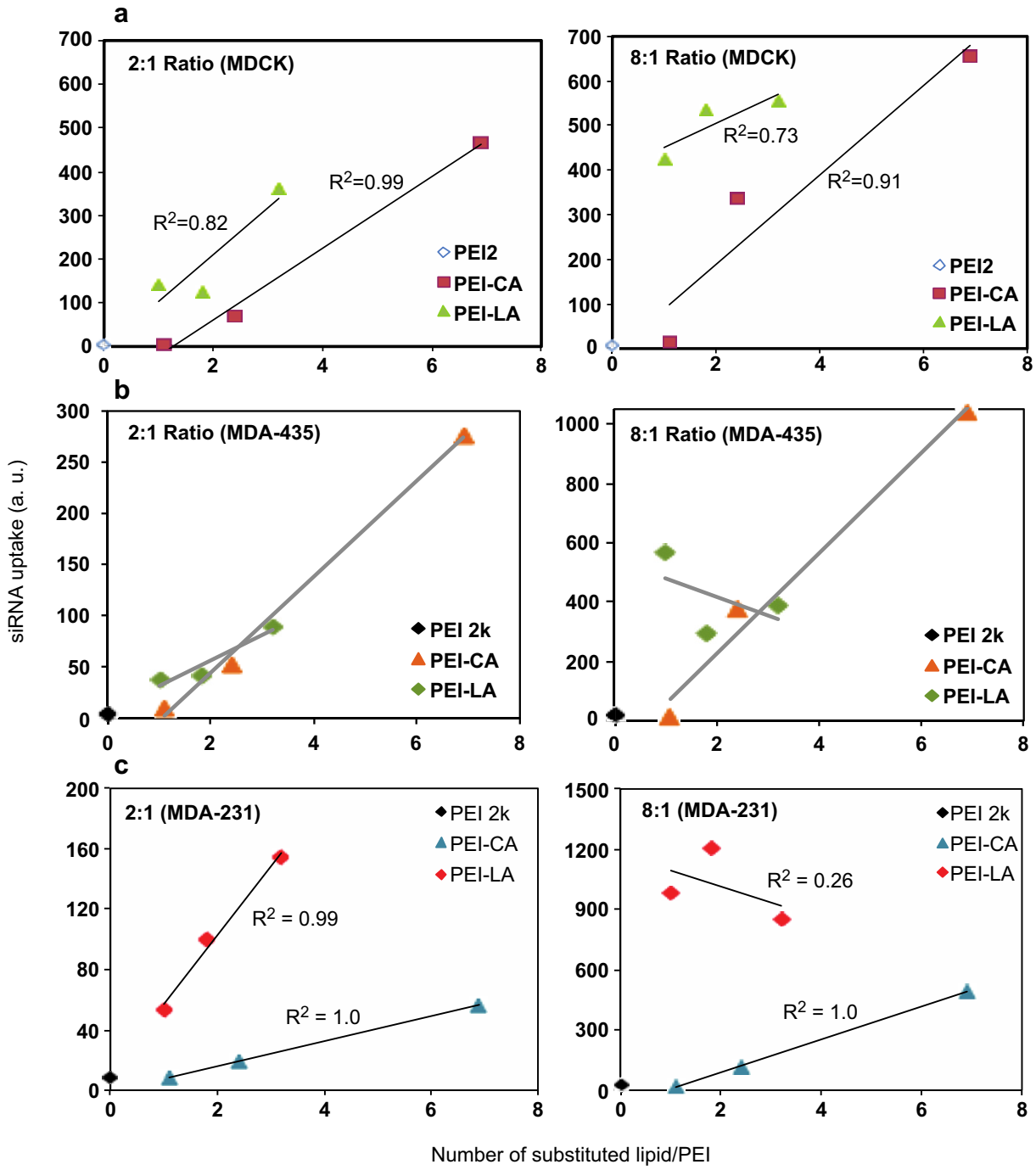

Fig. 10. The siRNA delivery into (a) MDCK, (b) MDA-435 and (c) MDA-231 cells with native and CA and LA substituted PEIs. The uptake was quantitated with FAM-labeled siRNAs and expressed in arbitrary fluorescence units. Experimental details on siRNA for MDCK, MDA-435 and MDA-231 cells can be found in References 12, 36, 37.

the stable lipid association are expected to be beneficial for internalization of the polyplexes through cell membranes, supporting the experimentally observed higher cellular uptake obtained with lipid modified carriers [9,12]. On the other hand, the peripheral location of lipids also provides an opportunity for siRNA polyplexes towards an undesirable aggregation state via facilitated hydrophobic interactions. It will be useful to design systems where the lipid moieties are exposed to periphery only after contact with cell surfaces, so that cell penetration is enhanced while aggregation in solution is suppressed. Also, the stable lipid association is undesired for the siRNA unloading at the target site. These opposing effects should be considered in rational design of lipid-modified polymer based carriers.

Our simulations can be adopted for investigating the complexation of siRNA molecules with other polycationic carriers. Through interpreting the structural properties of a siRNA polylex formed with a designed polycation, we can evaluate the siRNA complexation capability of this polycation from MD simulation. Future MD simulations can also be conducted to assess the performance of the polycation in releasing the delivered siRNA, thus helping to better interpret the experimental results on silencing efficiency and eventually helping screen candidate design schemes.

4. Conclusions

We performed a series of all-atom MD simulations to study siRNA complexation mediated by native and lipid-modified PEIs. We found that the lipid modification does not affect PEI's capability to neutralize the siRNAs. All five PEIs used in the simulations can completely neutralize the siRNAs at a distance of ~8 Å from the siRNA C1′ atoms. Polyion bridging plays an important role in siRNA complexation, which is not affected by the substituted lipids. The lipophilic moieties are located further away from the siRNAs compared to the cationic moieties. The lipid associations between short lipids (CA) form and break frequently for one and three CA substituted PEI. The lipid associations between long lipids (LA) are more stable, where the lipid associations never break once they form during the simulation for three LA substituted PEI. The results also revealed that siRNA structures mediated by lipid modified PEIs are more compact and stable. For PEIs modified with short lipids (CA), increasing the lipid substitution level from one to three lipids per PEI makes the effects of lipid modification manifest more dramatically, resulting in more compact and stable siRNA structure. For PEIs modified with long lipids (LA), increasing the lipid substitution from one to three lipids per PEI does not change the amount of PEI linkage via lipid association much, and it has a reverse effect on compacting siRNA structure due to increased steric hindrance brought by the lipid association among the three lipids on individual PEIs.

Acknowledgments

We thank Dr. Hamidreza M. Aliabadi for providing the cellular uptake data on siRNA complexes. We acknowledge the computing resources and technical support from Compute Canada and the high performance computing facility at the National Institute for Nanotechnology, Edmonton, Canada. This work was supported by the Natural Sciences and Engineering Research Council of Canada, Alberta Innovates – Technology Futures, and Canada Foundation for Innovation.

Appendix A. Supplementary data

Supplementary data related to this article can be found at http://dx.doi.org/10.1016/j.biomaterials.2013.01.011.

References

[1] Elbashir S, Harborth J, Lendeckel W, Yalcin A, Weber K, Tuschl T. Duplexes of 21-nucleotide RNAs mediate RNA interference in cultured mammalian cells. Nature 2001;411:494–8.
[2] Castanotto D, Rossi JJ. The promises and pitfalls of RNA-interference-based therapeutics. Nature 2009;457(7228):426–33.
[3] Boussif O, Lezoualc'h F, Zanta MA, Mergny MD, Scherman D, Demeneix B, et al. A versatile vector for gene and oligonucleotide transfer into cells in culture and in vivo: polyethylenimine. Proc Natl Acad Sci U S A 1995;92(16):7297–301.
[4] Godbey W, Wu K, Mikos A. Poly(ethylenimine) and its role in gene delivery. J Control Release 1999;60(2–3):149–60.
[5] Aliabadi HM, Landry B, Sun C, Tang T, Uludag H. Supramolecular assemblies in functional siRNA delivery: where do we stand? Biomaterials 2012;33(8):2546–69.
[6] Ledley F. Nonviral gene-therapy – the promise of genes as pharmaceutical products. Hum Gene Ther 1995;6(9):1129–44.
[7] Luo D, Saltzman W. Synthetic DNA delivery systems. Nat Biotechnol 2000;18:33–7.
[8] Incani V, Lavasanifar A, Uludag H. Lipid and hydrophobic modification of cationic carriers on route to superior gene vectors. Soft Matter 2010;6(10):2124–38.
[9] Abbasi M, Aliabadi HM, Moase EH, Lavasanifar A, Kaur K, Lai R, et al. siRNA-mediated down-regulation of P-glycoprotein in a xenograft tumor model in NOD-SCID mice. Pharm Res 2011;28(10):2516–29.
[10] Abbasi M, Lavasanifar A, Berthiaume LG, Weinfeld M, Uludag H. Cationic polymer-mediated small interfering RNA delivery for P-glycoprotein down-regulation in tumor cells. Cancer 2010;116(23):5544–54.
[11] Kim WJ, Chang CW, Lee M, Kim SW. Efficient siRNA delivery using water soluble lipopolymer for anti-anglogenic gene therapy. J Control Release 2007;118(3):357–63.
[12] Aliabadi HM, Landry B, Bahadur RK, Neamnark A, Suwantong O, Uludag H. Impact of lipid substitution on assembly and delivery of siRNA by cationic polymers. Macromol Biosci 2011;11(5):662–72.
[13] Ouyang D, Zhang H, Herten DP, Parekh HS, Smith SC. Structure, dynamics, and energetics of siRNA-cationic vector complexation: a molecular dynamics study. J Phys Chem B 2010;114(28):9220–30.
[14] Ouyang D, Zhang H, Parekh HS, Smith SC. Structure and dynamics of multiple cationic vectors-siRNA complexation by all-atomic molecular dynamics simulations. J Phys Chem B 2010;114(28):9231–7.
[15] Pavan GM, Albertazzi L, Danani A. Ability to adapt: different generations of PAMAM dendrimers show different behaviors in binding siRNA. J Phys Chem B 2010;114(8):2667–75.
[16] Pavan GM, Posocco P, Tagliabue A, Maly M, Malek A, Danani A, et al. PAMAM dendrimers for siRNA delivery: computational and experimental insights. Chem – Eur J 2010;16(26):7781–95.
[17] Pavan GM, Mintzer MA, Simanek EE, Merkel OM, Kissel T, Danani A. Computational insights into the interactions between DNA and siRNA with "rigid" and "flexible" triazine dendrimers. Biomacromolecules 2010;11(3):721–30.
[18] Pavan GM, Kostiainen MA, Danani A. Computational approach for understanding the interactions of UV-degradable dendrons with DNA and siRNA. J Phys Chem B 2010;114(17):5686–93.
[19] Vasumathi V, Maiti PK. Complexation of siRNA with dendrimer: a molecular modeling approach. Macromolecules 2010;43(19):8264–74.
[20] Jensen LB, Mortensen K, Pavan GM, Kasimova MR, Jensen DK, Gadzhyeva V, et al. Molecular characterization of the interaction between siRNA and PAMAM G7 dendrimers by SAXS, ITC, and molecular dynamics simulations. Biomacromolecules 2010;11(12):3571–7.
[21] Case DA, Darden TA, Cheatham I TE, Simmerling CL, Wang J, Duke RE, et al. AMBER 10. San Francisco: University of California; 2008.
[22] Sun C, Tang T, Uludag H. Molecular dynamics simulations for complexation of DNA with 2 kDa PEI reveal profound effect of PEI architecture on complexation. J Phys Chem B 2012;116(8):2405–13.
[23] Utsuno K, Uludag H. Thermodynamics of polyethylenimine-DNA binding and DNA condensation. Biophys J 2010;99(1):201–7.
[24] Humphrey W, Dalke A, Schulten K. VMD – visual molecular dynamics. J Mol Graph 1996;14:33–8.
[25] Phillips J, Braun R, Wang W, Gumbart J, Tajkhorshid E, Villa E, et al. Scalable molecular dynamics with NAMD. J Comput Chem 2005;26:1781–802.
[26] Sun C, Tang T, Uludag H, Cuervo JE. Molecular dynamics simulations of DNA/PEI complexes: effect of PEI branching and protonation state. Biophys J 2011;100(11):2754–63.
[27] Vanommeslaeghe K, Hatcher E, Acharya C, Kundu S, Zhong S, Shim J, et al. CHARMM general force field: a force field for drug-like molecules compatible with the CHARMM all-atom additive biological force fields. J Comput Chem 2010;31(4):671–90.
[28] Brooks BR, Bruccoleri RE, Olafson DJ, States DJ, Swaminathan S, Karplus M. CHARMM: a program for macromolecular energy, minimization, and dynamics calculations. J Comput Chem 1983;4:187–217.
[29] MacKerel Jr AD, Brooks III CL, Nilsson L, Roux B, Won Y, Karplus M. In: Schleyer P v R, et al., editors. CHARMM: the energy function and its parameterization with an overview of the program. Vol. 1 of the encyclopedia of computational chemistry. Chichester: John Wiley & Sons; 1998. p. 271–7.
[30] Jorgensen W. Quantum and statistical mechanical studies of liquids. 10. Transferable intermolecular potential functions for water, alcohols, and ethers – application to liquid water. J Am Chem Soc 1981;103:335–40.
[31] Darden T, York D, Pedersen L. Particle mesh ewald – an n.log(n) method for ewald sums in large systems. J Chem Phys 1993;98:10089–92.
[32] Ryckaert J, Ciccotti G, Berendsen H. Numerical-integration of cartesian equations of motion of a system with constraints – molecular-dynamics of n-alkanes. J Comput Phys 1977;23(3):327–41.
[33] Dunitz J. The entropic cost of bound water in crystals and biomolecules. Science 1994;264(5159):670.
[34] Sun C, Tang T, Uludag H. Molecular dynamics simulations of PEI mediated DNA aggregation. Biomacromolecules 2011;12:3698–707.
[35] Thomas AS, Elcock AH. Direct measurement of the kinetics and thermodynamics of association of hydrophobic molecules from molecular dynamics simulations. J Phys Chem Lett 2011;2(1):19–24.
[36] Aliabadi HM, Landry B, Mandipoor P, Hsu CYM, Uludag H. Effective down-regulation of breast cancer resistance protein (BCRP) by siRNA delivery using lipid-substituted aliphatic polymers. Eur J Pharm Biopharm 2012;81(1):33–42.
[37] Aliabadi HM, Landry B, Mandipoor P, Uludag H. Induction of apoptosis by survivin silencing through siRNA delivery in a human breast cancer cell line. Mol Pharm 2011;8(5):1821–30.
[38] Waite CL, Sparks SM, Uhrich KE, Roth CM. Acetylation of PAMAM dendrimers for cellular delivery of siRNA. BMC Biotechnol 2009;9(38).
[39] Suma T, Miyata K, Ishii T, Uchida S, Uchida H, Itaka K, et al. Enhanced stability and gene silencing ability of siRNA-loaded polyion complexes formulated from polyaspartamide derivatives with a repetitive array of amino groups in the side chain. Biomaterials 2012;33(9):2770–9.